Micro-T Circuit Model for the Analysis of Cylindrical Induction Heating Systems

Layth Jameel Buni Qaseer

***Abstract*—A method is given for obtaining a phase terminal equivalent circuit, which is useful for the analysis of cylindrical induction heating systems for electric energy conversion into heat. The excitation is circumferential and can be realized as either a three-phase system or a single-phase system. The iterative form of the solution allows for solid and hollow charges. First, a general form of the field solution is obtained using transfer matrices. A variable transformation is then made, which makes it possible to derive an equivalent circuit for each annular region in the system. By joining the equivalent circuits in cascade, an equivalent circuit for the complete system is obtained. The voltages and currents in the equivalent circuit relate directly to the field quantities within the actual system.**

***Index Terms*—Eddy currents, electromagnetic induction, energy conversion, equivalent circuits, induction heating.**

I. Introduction

INDUCTION heating is the use of the principle of electromagnetic induction for the conversion of electrical energy into thermal energy to achieve various heating applications. This method of heating metals is preferred in comparison with other methods for many reasons such as its shorter time spent to heat the charge, no combustion products, accurate temperature control, possibility to give uneven taper heating. The basic induction heating system (IHS) to be analyzed consists of a cylindrical charge surrounded by an exciting coil; therefore, the system can be considered as a multilayer cylindrical system.

Different numerical methods have been developed in 2-D and 3-D for the analysis of IHS. Among these methods, the finite element method (FEM) and the boundary element method (BEM) are the most popular [1]–[3]. A hybrid method based on the coupling of FEM and BEM has been found advantageous for unbounded field problems [4]–[6]. Ismail and Marzouk [7] used the iterative hybrid FEM–BEM for the analysis of IHS with nonlinear charge.

The aim of this paper is to show how the analytical solution to the field problem may be extended to yield an equivalent circuit representation for the IHS. An attempt is made to show the unification of field and circuit theory.

Manuscript received November 26, 2009; revised February 13, 2010; accepted March 21, 2010. Date of publication August 23, 2010; date of current version November 19, 2010. This work was supported in part by the German Academic Exchange Service (DAAD) under Grant A0901170. Paper no. TEC-00501-2009.

The author is with the General and Theoretical Electrical Engineering Department, University of Duisburg-Essen, Duisburg D-47048, Germany (e-mail: layth.qaseer@uni-duisburg-essen.de).

Color versions of one or more of the figures in this paper are available online at http://ieeexplore.ieee.org.

Digital Object Identifier 10.1109/TEC.2010.2046642

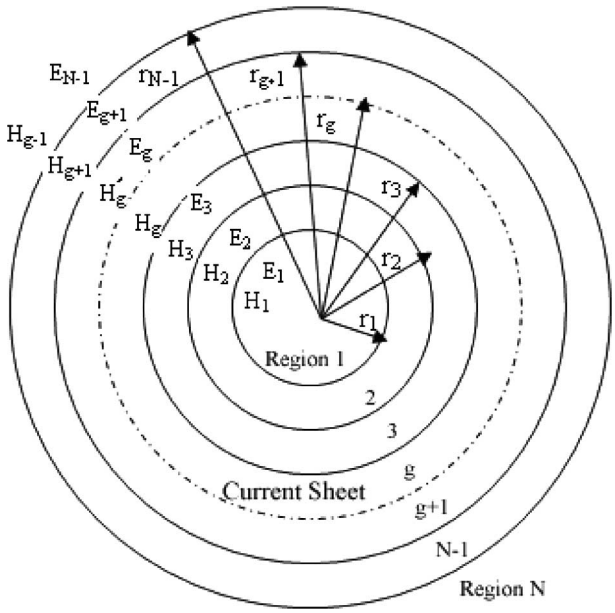

Fig. 1. Cross section through cylindrical multilayer IHS.

It is usually straightforward to relate field quantities in the system to voltages and currents in the equivalent circuits. The approach in this paper is presented along a simple and feasible multiregion model.

A region is defined as an area in the system in which the material is uniform in nature, having boundaries of simple cylindrical shape.

The equivalent circuits developed here have the form of cascaded transmission lines; therefore, it is possible to consider any number of regions without recourse to lengthy analysis.

The accuracy of the method is verified with measurements of practical IHS together with comparisons to numerical and analytical methods.

II. Mathematical Model

A general multiregion problem is analyzed. Fig. 1 shows a cross section of an IHS comprising N infinitely long concentric cylinders with a radially infinitesimally thin and axially infinite current sheet excitation at radius r_g. It is further assumed that displacement currents and the magnetic saturation are negligible.

The important field quantities are those acting at the region boundaries. For the models considered here, there are at most three field quantities that are relevant. These are the electric field strength E, which is directed circumferentially along the interface, the magnetic field strength *H,* which is directed axially

along the interface, and the third one at both ends of the pole pitch, if existing, is the flux density B normal to the interface. The analysis of the aforementioned Azimuthal, axial, and radial electromagnetic field components are performed to obtain the field quantities at the proper interfaces between the regions. If these quantities are known, the equivalent circuit is then derived as well as the power flow through the interfaces and the driving electromagnetic force (in the case of traveling wave IHS [TWIHS] with three-phase excitation).

The intermediate stage between the field solution and the final equivalent circuit is represented in a transmission line form [8]. It was well known that the E and H values on either side of a region could be linked by a transfer matrix [9]–[11]. Hence, every bounded region in the model shown in Fig. 1 could be represented by a corresponding transfer matrix equation.

In the following sections, the theoretical analysis for three-phase and single-phase excitations are derived.

III. Theoretical Analysis for the Three-Phase Model

It is assumed that the winding produces a perfect sinusoidal traveling wave. The line current density may be represented as

$$J_\theta = \mathrm{Re}\left[J' \exp\left\{j(\omega t - kz)\right\}\right] \tag{1}$$

where J', ω, and k are the amplitude of line current density, angular frequency, and wavelength factor, respectively, where the latter is related to the pole pitch τ by

$$k = \pi/\tau. \tag{2}$$

A. Field Theory Solution

The field produced will link all cylindrical regions from 1 to N. Maxwell's equations are solved accordingly [11] to yield (for regions $1 < n < N$)

$$\begin{bmatrix} E_{\theta,n} \\ H_{z,n} \end{bmatrix} = [T_n] \cdot \begin{bmatrix} E_{\theta,n-1} \\ H_{z,n-1} \end{bmatrix} \tag{3}$$

where $E_{\theta,n}$ and $H_{z,n}$ are the field components at the outer boundary of region n and $E_{\theta,n-1}$ and $H_{z,n-1}$ are the equivalent values at the inner boundary of the same region and $[T_n]$ is the associated transfer matrix [9], [12], which is given by

$$[T_n] = \begin{bmatrix} a_n & b_n \\ c_n & d_n \end{bmatrix}. \tag{4}$$

Expressions for a_n, b_n, c_n, and d_n are provided in the Appendix. Hence, given the values of E_θ and H_z at the inner boundary of a region, the values of E_θ and H_z at the outer boundary are immediately obtainable from this simple transfer matrix relation. At the boundaries, where no excitation current sheet exists, E_θ and H_z are continuous; thus, for example, if two regions are considered with no current sheet at the common boundary, knowing E_θ and H_z at the inner boundary of the first region, E_θ and H_z at the outer boundary of the second region can be calculated by successive use of the underlying two transfer matrices. Considering the excitation current sheet to be at radius r_g, then

$$H'_{z,n} = H_{z,n} \text{ (in ampere per meter)}, \qquad n \neq g \tag{5}$$

and

$$H'_{z,n} = H_{z,n} - J' \text{ (in ampere per meter)}, \qquad n = g \tag{6}$$

where $H_{z,n}$ is the axial magnetic field strength in close inner proximity to the boundary and $H'_{z,n}$ is the axial magnetic field strength in close outer proximity to the boundary.

Given the current sheet excitation at radius r_g, the overall structure divides into an outer part, which is modeled according to

$$\begin{bmatrix} E_{\theta,n-1} \\ H_{z,n-1} \end{bmatrix} = [T_{n-1}] \cdot [T_{n-2}] \ldots [T_{g+1}] \cdot \begin{bmatrix} E_{\theta,g} \\ H_{z,g} - J' \end{bmatrix} \tag{7}$$

and an inner part, which supports the following relation:

$$\begin{bmatrix} E_{\theta,g} \\ H_{z,g} \end{bmatrix} = [T_g] \cdot [T_{g-1}] \ldots [T_2] \cdot \begin{bmatrix} E_{\theta,1} \\ H_{z,1} \end{bmatrix}. \tag{8}$$

Enough information is now available to find all field components; hence, the equivalent circuit model can be set up using the surface impedances of the regions under consideration.

B. Surface Impedance Calculations

Looking outward from the current sheet, the surface impedance at a boundary of radius r_n is defined as

$$Z_{n+1} = \frac{E_{\theta,n}}{H_{z,n}} \tag{9}$$

and the surface impedance looking inward is defined as

$$Z_n = -\frac{E_{\theta,n}}{H_{z,n}}. \tag{10}$$

Using the method obtained in [11] with the values of $E_{\theta,N-1}$, $H_{z,N-1}$, $E_{\theta,1}$, $H_{z,1}$, and a_n, b_n, c_n, and d_n as derived in the previous section, then

$$Z_{\mathrm{in}} = \frac{Z_g \cdot Z_{g+1}}{Z_g + Z_{g+1}} \tag{11}$$

where Z_{in} is the input surface impedance at the current sheet, and Z_{g+1} and Z_g are the surface impedances looking outward and inward at the current sheet. Substituting for Z_g and Z_{g+1} using (10) and (9), respectively, and rearranging the terms yields

$$Z_{\mathrm{in}} = -\frac{E_{\theta,g}}{H_{z,g} - H'_{z,g}}. \tag{12}$$

Substituting now (6) into (12) provides the following simple relation:

$$Z_{\mathrm{in}} = -\frac{E_{\theta,g}}{J'}. \tag{13}$$

From this, the input surface impedance at the current sheet can be determined. All the field components can be found by a straightforward use of this and (7), (8), and (10).

Having found E_θ and H_z at all boundaries, it is then a simple matter to calculate the power entering a region through the concept of Poynting vector. The time-average power P_{in} passing through a surface is usually given as

$$P_{\mathrm{in}} = \frac{1}{2}\mathrm{Re}\{\bar{E} \times \bar{H}^*\} \text{ (in watt per meter square)}. \tag{14}$$

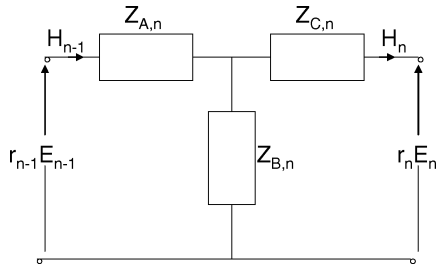

Fig. 2. Basic T-circuit for region n.

Using (10) and (13), it can be shown that the total power per axial unit length is

$$P_w = 0.5\,|E_{\theta,g}|^2\,\mathrm{Re}\left\{\frac{2\pi r_g}{Z_{\mathrm{in}}}\right\}\ \text{(in watt per meter)}. \tag{15}$$

It is, therefore, a simple matter to calculate the driving electromagnetic force per axial unit length, e.g., for stirring and heal melting purposes

$$F_z = \frac{P_w}{2\tau f}\ \text{(in newton per meter)} \tag{16}$$

where f is the operating frequency.

As the transfer matrix formalism is strictly rooted in the analytical field solutions, the presented formalism might be regarded as sufficient in itself. However, from the technical viewpoint, it is hardly possible to draw a clear picture that refers to any of the intended functionalities. Engineers, for most of the part, prefer to think in terms of an equivalent circuit model rather than to refer to full-wave time-varying field analysis. In addition, the impact of altering design parameters is easier to grasp than in the framework of an applied electromagnetics analysis. For this reason, an equivalent circuit model has been developed in the following section.

C. The Micro-T Terminal Equivalent Circuit

The underlying transmission-line form of (5)–(7) suggests that, by analogy, some form of equivalent circuit is possible [10], [13]. No loss of generality occurs, if only one region is considered. The electric and magnetic field quantities are linked as shown in (3). In order to represent the relationship between E_n, H_n and E_{n-1}, H_{n-1} by a corresponding T-circuit, a change of variable is required. Without such a transformation, it does not appear to be possible to represent a region with such a simple three-element circuit. A practical variable transformation refers to the variable E, which is changed to *rE* [14].

A T-circuit can now be used to link the variables *rE* and H on either side of a region as shown in Fig. 2.

In effect, the current H_n in a T-circuit is driven by a voltage $r_n E_n$. For the general region n, the impedances are given by the following relations:

$$Z_{B,n} = -\frac{r_{n-1}}{c_n} \tag{17}$$

$$Z_{A,n} = Z_{B,n}[d_n - 1] \tag{18}$$

$$Z_{C,n} = Z_{B,n}\left[a_n \frac{r_n}{r_{n-1}} - 1\right]. \tag{19}$$

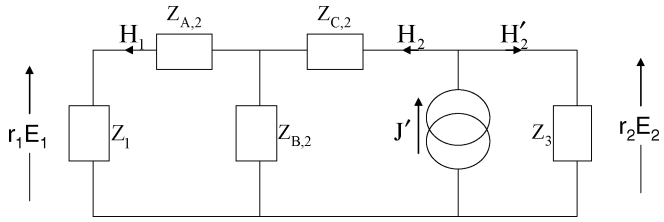

Fig. 3. Basic equivalent circuit for a three-region IHS.

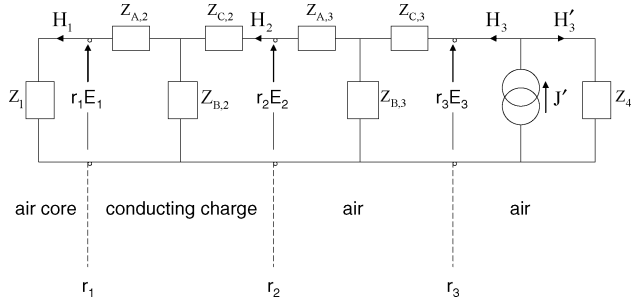

Fig. 4. Equivalent circuit for a hollow charge IHS.

On joining the T-circuits in cascade, the full basic equivalent circuit for, e.g., a three-region IHS is obtained as shown in Fig. 3, representing an IHS with a solid charge, where by using (9) and (10), the following expressions are obtained [13], [14]:

$$Z_1 = -\frac{r_1 E_1}{H_1} \tag{20}$$

$$Z_3 = \frac{r_2 E_2}{H_2'}. \tag{21}$$

Thus, an equivalent circuit has been derived by a rearrangement of the field solution, where the voltages and currents are directly related to the field quantities. Furthermore, the normal flux density at any interface can be obtained in the form

$$B_{r,n} = \frac{E_{\theta,n}}{2\tau f}. \tag{22}$$

It is worth noting that for a hollow charge IHS, the number of regions is increased by 1, where region 1 now represents the air core of the charge as shown in Fig. 4.

It is convenient to think in terms of phase voltages and currents. The input quantities to the basic equivalent circuit are the current J' and the voltage $2\pi r_g E_g$. The relation between J' and the rms. phase current I can be written as

$$J' = \frac{6\sqrt{2} N_{\mathrm{eff}} I}{\tau p}\ \text{(in ampere per meter)} \tag{23}$$

where p is the number of poles and N_{eff} stands for the effective number of series turns per phase, hence,

$$I = (I_{\mathrm{fac}})J'. \tag{24}$$

The phase voltage is linked to $2\pi r_g E_g$ by

$$V = 2\sqrt{2}\pi N_{\text{eff}} r_g E_g \tag{25}$$

therefore,

$$V = V_{\text{fac}} r_g E_g. \tag{26}$$

Let us now consider the effect of multiplying the quantities $r_n E_n$ and H_n terms in the basic equivalent circuit by the factors V_{fac} and I_{fac}, respectively, then the impedances in the basic circuit have to be multiplied by an impedance factor given by

$$Z_{\text{fac}} = \frac{V_{\text{fac}}}{I_{\text{fac}}} = \frac{24(N_{\text{eff}})^2}{\tau p} \tag{27}$$

and the terminal impedance of the IHS is given by

$$Z_t = Z_{\text{fac}} r_g Z_{\text{in}} \text{ (in ohm)}. \tag{28}$$

This relation results in a completely new equivalent circuit in which the input quantities are the rms voltage and rms current, using (25) and (24). Thus, the various voltages and currents at the input to each T-circuit are now related directly to the field quantities at the corresponding interfaces of IHS and this terminal equivalent circuit has all the advantages of the basic circuit, but, in addition, the impedances are real impedances.

IV. Theoretical Analysis for the Single-Phase Model

A. Field Theory Solution

The analysis of a single-phase model is much simpler than the evaluation of the three-phase model because only regions inside the current sheet need to be considered, namely, the regions $g+1$ to N do not affect the field distribution [15] in any way. The excitation is provided by a single continuous coil carrying alternating current. The line current density takes the form

$$J_\theta = \text{Re}\{J' \exp(j\omega t)\}. \tag{29}$$

In this case, $k = 0$, all field relations hold. The input surface impedance at the current sheet becomes

$$Z_{\text{in}} = Z_g \tag{30}$$

where Z_g is obtained by applying (10)

If region n has an infinite resistivity, then the expressions for a_n, b_n, c_n, and d_n are modified and given in Appendix.

B. The Micro-T Terminal Equivalent Circuit

For a single-phase IHS with a solid charge comprising three regions, region 1 being the charge, the T-circuit for the second region (which is air) is reduced to single-series impedance due to infinite penetration depth [14], as shown in Fig. 5. This impedance is determined in the following:

$$Z_{\text{AC},2} = -b_2 r_2. \tag{31}$$

For region 1, which represents the solid charge, only a single impedance termination is necessary. This is linked to the surface impedance Z_1' of region 1 by the expression [11]

$$Z_1 = r_1 Z_1' = r_1 \frac{j\omega\mu_1}{\alpha_1} \frac{I_1(\alpha_1 r_1)}{I_0(\alpha_1 r_1)} \tag{32}$$

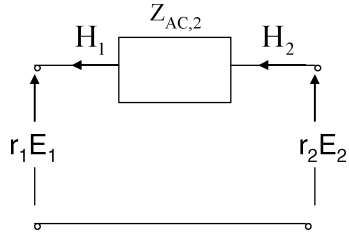

Fig. 5. T-circuit for a nonconducting region (shunt impedance infinite).

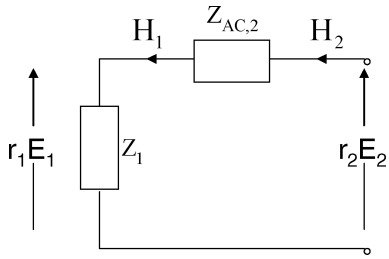

Fig. 6. Basic Equivalent circuit for a solid charge single-phase IHS.

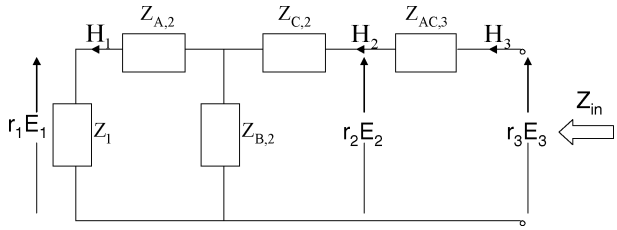

Fig. 7. Basic Equivalent circuit for a hollow charge single-phase IHS.

where μ_1 and σ_1 are the permeability and conductivity of region 1. I_1 and I_0 are the modified Bessel's functions of the first kind and of order 1 and 0, respectively. The attenuation constant α_1 is defined by

$$\alpha_1 = (j\omega\alpha_1\mu_1)^{1/2}. \tag{33}$$

Hence, the basic equivalent circuit for the three-region problem can be set up as shown in Fig. 6.

For a hollow charge IHS, there are four regions, three of which are inside the current sheet. The various impedances of the T-circuit for a conducting region are given by (17)–(19). The corresponding equivalent circuit is shown in Fig. 7.

If there are N turns per axial unit length, then the voltage per axial unit length applied to the solenoid is given by

$$V = \sqrt{2} N \pi r_g E_g. \tag{34}$$

Similarly, J' and I are linked by the relationship

$$J' = \sqrt{2} N I \text{ (in ampere per meter)} \tag{35}$$

and the terminal impedance per axial unit length of the solenoid amounts to

$$Z_t = \frac{V}{I} = 2\pi N^2 r_g Z_{\text{in}} \tag{36}$$

where Z_{in} is the input impedance defined in (30). This quantity multiplied by the impedance factor yields the solenoid impedance per unit length as given in (36).

TABLE I
DESIGN PARAMETERS OF THE PRACTICAL IHS (BASED ON [16, Ex. 9])

Coil inner diameter, (m)	0.08256
Coil length, (m)	0.254
Number of turns	29
Exciting field intensity, (A/m)	95493 r.m.s
Frequency, (Hz)	60
Charge material	Steel SAE1045
Charge diameter, (m)	0.06032
Charge length, (m)	0.254
Charge conductivity, (S/m)	5.0×10^{6}
Charge relative permeability	18

Now, if all impedances in the basic equivalent circuit are multiplied by the impedance factor, the terminal equivalent circuit is obtained. The input impedance to this second form of circuit is then the impedance per unit length of the solenoid's axial extension. The voltages and currents appearing in the circuit can then be used in (34) and (35) in order to obtain the field quantities E and H at any desired region boundary.

V. NUMERICAL RESULTS

The equivalent circuit method that has been described in the earlier sections is validated along three examples. The first example consists of a practical single-phase IHS with nonlinear charge, which has been considered earlier by Stansel [16]. The importance of this example is that measurements are available in addition to calculations. The second example encompasses a numerical solution based on the finite difference method [17] for an IHS with both single-phase and three-phase excitations. The third example employs an analytical method for an IHS with a hollow charge [18]. For comparison reasons, FEM computation is adopted in our analysis, which is widely used as a numerical technique for this kind of applications.

In our implementation, the field domain is divided into a number of regions, each being defined by its coordinates, permeability, and conductivity. Each region is discretized using first-order triangular elements [19]. The induced power in the charge is obtained through the solution of governing differential equation for each nodal magnetic vector potential. Three values of power are computed: the power integrated over the coil, the air gap power, and the power integrated over the charge.

The solution is assumed to be convergent when these three values do not differ by more than 1%, which is then termed as the power mismatch or power imbalance.

A. Practical IHS

This problem has been considered by Stansel [16], where measurements of electrical parameters are given. The design parameters of the analyzed IHS are provided in Table I. A nonlinear charge with ferromagnetic properties is considered using the analysis procedure proposed in [7] along with a hybrid FEM simulation. Numerical results are obtained for the following two cases.

1) Assuming linear charge having constant relative permeability corresponding to the rms value of the field intensity at the charge surface.
2) Using the actual magnetic properties of the charge such as that given in [7].

The results are compared to the data obtained by the proposed micro-T circuit method as well as to our FEM analysis, showing a good agreement even with the measured data from [16] (see Table II).

TABLE II
COMPUTED PARAMETERS OF THE PRACTICAL SINGLE-PHASE IHS

parameter	measured value [16]	value computed by empirical formula [16]	FEM value case1	FEM value case2	Micro-T circuit value
Charge Resistance (Ω)	0.0135	0.0137	0.0097	0.0139	0.0167
Reactance (Ω)	0.025	0.020	0.0201	0.0235	0.0231

TABLE III
COMPUTED PARAMETERS OF THE PRACTICAL THREE-PHASE IHS

Parameter	FEM value Case 1	FEM value Case2	Micro-T circuit value
Per phase charge resistance (Ω)	7.874×10^{-4}	8.41×10^{-4}	8.146×10^{-4}
Per phase reactance (Ω)	3.506×10^{-3}	4.485×10^{-3}	3.7×10^{-3}
Charge power (W)	1596.98	1704.94	1652.11
Axial force	104.79	111.87	108.41

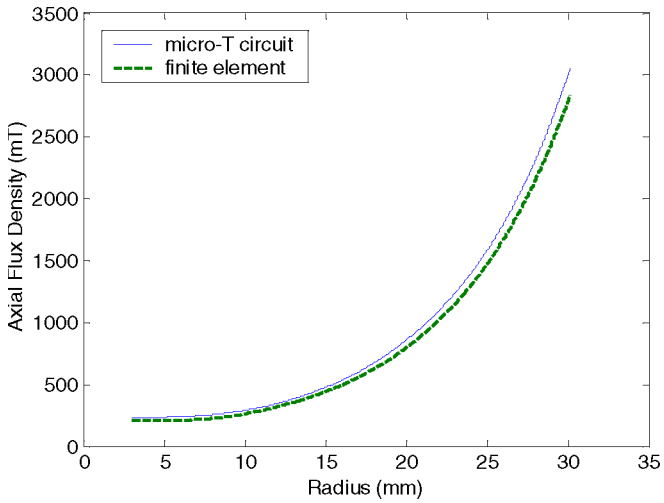

Fig. 8. Variation of axial flux density component with radius for single-phase excitation.

Table III shows the numerical results obtained for the same amplitude of line current density using three-phase excitation. Again the two methods correlate well.

Fig. 8 shows the variation of the axial magnetic flux density component with radius at the middle of coil axial length for single-phase excitation using FEM and micro-T circuit method. The agreement between the results of both methods may be considered good with a maximum relative deviation of 5%. Obviously, there is no radial component for single-phase IHS and this can be derived directly from Maxwell's equations.

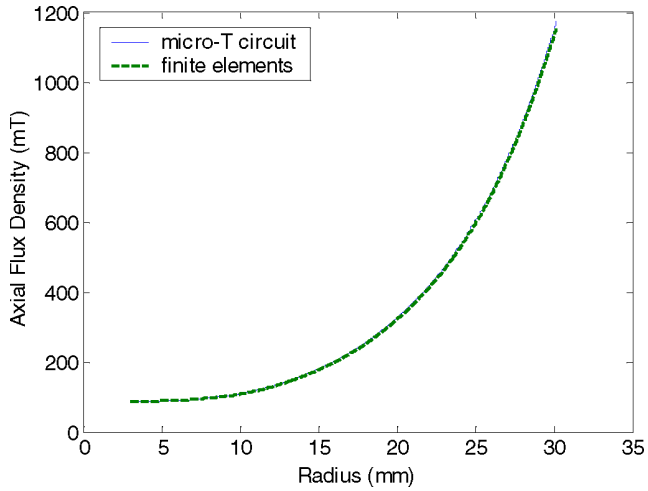

Fig. 9. Variation of axial flux density component with radius for three-phase excitation (two-pole connection).

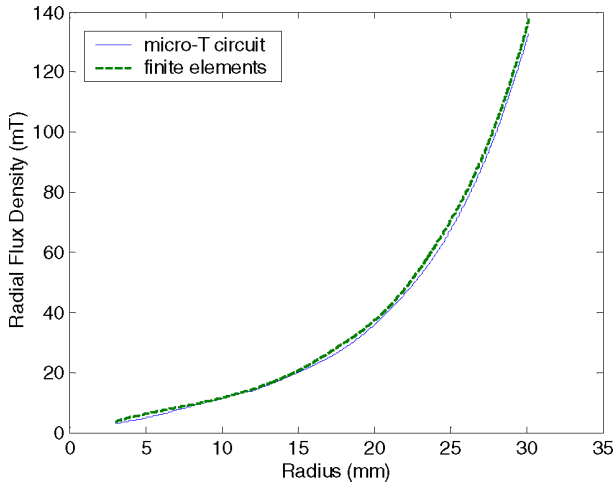

Fig. 10. Variation of radial flux density component with radius for three-phase excitation (two-pole connection).

Figs. 9 and 10 show, respectively, the radial profile of the axial and radial components of the magnetic flux density for the three-phase model with a two-pole connection. It is apparent that the axial component is larger than the radial one, since it is actually an axial flux machine, i.e., the pole pitch is larger than the diameter of the coil. The maximal relative deviation between the results of both methods amounts to only 3.5%.

B. Theoretical Polyphase Model

Reference [17] is adopted, since it deals with the numerical analysis of three-phase cylindrical IHS in addition to single-phase one among many configurations. The design parameters are given in Table IV. Two configurations are considered in the present study: the single-phase configuration and the three-phase configuration with two-pole connection. As in the preceding example, the same value of line current density amplitude is applied for both the cases.

Table V shows the numerical results obtained for this IHS model using two different configurations. It is apparent from the results that the proposed micro-T circuit method agrees well with the finite element analysis.

TABLE IV
DESIGN PARAMETERS FOR NUMERICAL MODEL OF IHS (BASED ON [17])

Coil inner diameter, (m)	0.6
Coil length, (m)	0.9
Amplitude of line current density, (kA/m)	100
Frequency, (Hz)	200
Inside crucible diameter, (m)	0.48
Outside crucible diameter, (m)	0.5
Crucible length, (m)	0.9
Crucible conductivity, (S/m)	0.9×10^{6}
Bath conductivity, (S/m)	0.933×10^{6}
Relative permeability of both crucible and bath	1

TABLE V
COMPUTED CHARGE POWER OF NUMERICAL INDUCTION HEATING MODEL [17], VALUES IN KW]

Excitation	Value computed by reference [17]	Value computed by reference [16]	FEM value	Micro-T circuit value
Single phase	145.3	177.4	164.6	190
Three phase-2 pole connection	117.5	—	84.8	86.6

TABLE VI
DESIGN PARAMETERS FOR A HOLLOW CHARGE MODEL (BASED ON [18, Ex. 12.9])

Coil length, (m)	0.5
Amplitude of line current density (kA/m)	100
Frequency, (Hz)	50
Charge thickness, (m)	10^{-4}
Charge outer diameter, (m)	0.25
Charge length, (m)	0.5
Charge conductivity, (S/m)	1.429×10^{6}
Relative permeability of the charge	1

TABLE VII
COMPUTED INDUCED POWER IN THE HOLLOW CHARGE MODEL (BASED ON [18, VALUES IN W])

Excitation	Value computed by reference [18]	FEM value	Micro-T circuit value
Single phase	170	150.2	170.57
Three phase-2 pole connection	—	44.39	46.7

C. IHS With Hollow Charge

This problem has been considered by Davies and Simpson [18], where an analytical method was used to compute the induced power within a hollow conducting cylinder excited by a single-phase supply. The corresponding design parameters of the analyzed system are given in Table VI.

As in the earlier section, the micro-T circuit method and FEM are compared with the analytical method in [18], using both single-phase and three-phase excitations with the same amplitude of line current density. Table VII displays the numerical results for this model. Again, the three models agree well.

VI. Conclusion

The micro-T circuit has been used for the analysis of cylindrical IHS for both single-phase and three-phase excitations. It can be used for any number of regions, and in addition, with any number of poles in the case of TWIHS so that our proposed method of analysis becomes quite general. Using such circuits may provide a better technical insight into the system than is possible from studying the full-wave solutions from a computational electromagnetics analysis.

Given just the voltages and currents in the terminal equivalent circuit, the field quantities at any region boundary can be easily derived.

The obtained results agree well with the data from the corresponding FEM analysis and also with the experimental data.

Appendix

1) Transfer matrix elements for three-phase excitation

$$a_n = \alpha_n r_{n-1}[I_1(\alpha_n r_n)k_0(\alpha_n r_{n-1}) + I_0(\alpha_n r_{n-1})k_1(\alpha_n r_n)] \quad (37)$$

$$b_n = j\omega\mu_n r_{n-1}\left[I_1\left(\alpha_n r_{n-1}\right)k_1\left(\alpha_n r_n\right) - I_1\left(\alpha_n r_n\right)k_1\left(\alpha_n r_{n-1}\right)\right] \quad (38)$$

$$c_n = j\frac{\alpha_n^2 r_{n-1}}{\omega\mu_n}[I_0(\alpha_n r_n)k_0(\alpha_n r_{n-1}) - k_0(\alpha_n r_n)I_0(\alpha_n r_{n-1})] \quad (39)$$

$$d_n = \alpha_n r_{n-1}[I_0(\alpha_n r_n)k_1(\alpha_n r_{n-1}) + k_0(\alpha_n r_n)I_1(\alpha_n r_{n-1})]. \quad (40)$$

where k_1 and k_0 are the modified Bessel's functions of the second kind and of order 1 and 0, respectively, and α is defined by the relation

$$\alpha^2 = k^2 + j\omega\mu\sigma.$$

Equations (37)–(40) also apply for single-phase excitation with $\sigma_n \neq 0$, where σ_n is the conductivity of region n.

2) Transfer matrix elements for single-phase excitation with $\sigma_n = 0$

$$a_n = \frac{r_{n-1}}{r_n} \quad (41)$$

$$b_n = -\frac{j\omega\mu_n}{2r_n}\left(r_n^2 - r_{n-1}^2\right) \quad (42)$$

$$c_n = 0 \quad (43)$$

$$d_n = 1. \quad (44)$$

Acknowledgment

The author would like to thank D. Erni, his host, and coworker at the university of Duisburg-Essen for advice and encouragement.

References

[1] J. Donea, S. Giuliano, and A. Philippe, "Finite elements in the solution of electromagnetic induction problems," *Int. J. Numerical Methods Eng.*, vol. 8, pp. 359–367, 1974.

[2] K. Ishibashi, "Analysis of induction heating characteristics by the boundary element method," *Electr. Eng. Jpn.*, vol. 108, no. 1, pp. 101–109, 1988.

[3] T. H. Fawzi, K. F. Ali, and P. E. Bruke, "Boundary integral equations analysis of induction devices with rotational symmetry," *IEEE Trans. Magn.*, vol. MAG-19, no. 1, pp. 36–44, Jan. 1983.

[4] S. J. Salon and J. D'Angelo, "Applications of the hybrid finite element-boundary element method in electromagnetics," *IEEE Trans. Magn.*, vol. MAG-24, no. 1, pp. 80–85, Jan. 1988.

[5] T. Miyoshi, M. Sumiya, and H. Omori, "Analysis of an induction heating system by the finite element method combined with a boundary integral equation," *IEEE Trans. Magn.*, vol. MAG-23, no. 2, pp. 1827–1832, Mar. 1987.

[6] F. Matsuoka and A. Kameari, "Calculation of three dimensional eddy current by FEM-BEM coupling method," *IEEE Trans. Magn.*, vol. MAG-24, no. 1, pp. 182–185, Jan. 1988.

[7] K. S. Ismail and R. A. Marzouk, "Iterative hybrid finite element-boundary element method for the analysis of induction heating system with nonlinear charge," *IEEE Trans. Magn.*, vol. 32, no. 4, pp. 3212–3218, Jul. 1996.

[8] A. I. Cullen and T. H. Barton, "A simplified electromagnetic theory of the induction motor using the concept of wave impedance," *Proc. IEE*, vol. 150C, pp. 331–336, 1959.

[9] J. Greig and E. M. Freeman, "Traveling wave problem in electrical machine," *Proc. IEE*, vol. 114, no. 11, pp. 1681–1683, 1967.

[10] E. M. Freeman, "Traveling waves in induction machines: input impedance and equivalent circuits," *Proc. IEE*, vol. 115, no. 12, pp. 1772–1776, Dec. 1968.

[11] E. M. Freeman and B. E. Smith, "Surface impedance method applied to multilayer cylindrical induction devices with circumferential exciting currents," *Proc. IEE*, vol. 117, no. 10, pp. 2012–2013, Oct. 1970.

[12] L. A. Pipes, "Matrix theory of skin effect on laminations," *J. Franklin Inst.*, vol. 262, pp. 127–138, 1956.

[13] E. M. Freeman, "Equivalent circuits from electromagnetic theory: Low frequency induction devices," *Proc. IEE*, vol. 121, no. 10, pp. 1117–1121, 1974.

[14] E. M. Freeman and T. G. Bland, "Equivalent circuit of concentric cylindrical conductors in an axial alternating magnetic field," *Proc. IEE*, vol. 123, no. 2, pp. 149–152, 1976.

[15] L. J. Bunni and K. Altaii, "The layer theory approach applied to induction heating systems with rotational symmetry," in *Proc. IEEE Southeastcon*, Richmond, VA, Mar. 2007, pp. 413–420.

[16] N. R. Stansel, *Induction Heating*, 1st ed. New York: McGraw-Hill, 1949.

[17] V. Fireteanu and R. Gheysens, "Numerical modeling of the traveling field diffusion. Induction heating and electromagnetic stirring," *IEEE Trans. Magn.*, vol. 28, no. 2, pp. 1489–1492, Mar. 1992.

[18] J. Davies and P. Simpson, *Induction Heating Handbook*. London, U.K.: McGraw-Hill, 1979.

[19] S. J. Salon, *Finite Element Analysis of Electrical Machines*. Norwell, MA: Kluwer, 1995.

Layth Jameel Buni Qaseer was born in Baghdad, Iraq, on October 13, 1957. He received the B.Sc., M.Sc., and Ph.D. degrees from the University of Baghdad, Baghdad, in 1979, 1993, and 2004, respectively, all in electrical engineering.

During 2005, he was in the Mechatronic Engineering Department, University of Baghdad. He is currently at General and Theoretical Electrical Engineering Department, University of Duisburg-Essen, Duisburg, Germany. His current research interests include rotary, flat linear, tubular linear induction motors, helical motion induction motors as well as induction heating.